# Metadata of the article that will be visualized in OnlineFirst

| | | |
|---|---|---|
| ArticleTitle | Synthesis of resin from Alfa stem to applied as an adhesive corrosion-resistant coating | |
| Article Sub-Title | | |
| Article CopyRight | Indian National Science Academy<br>(This will be the copyright line in the final PDF) | |
| Journal Name | Proceedings of the Indian National Science Academy | |
| Corresponding Author | FamilyName | **Safi** |
| | Particle | |
| | Given Name | **Brahim** |
| | Suffix | |
| | Division | Research Unit: Materials, Processes and Environment, Faculty of Technology |
| | Organization | M'hamed Bougara University -Boumerdes |
| | Address | 35000, Boumerdes, Algeria |
| | Phone | |
| | Fax | |
| | Email | safi_b73@univ-boumerdes.dz |
| | URL | |
| | ORCID | http://orcid.org/0000-0003-2565-8135 |
| Author | FamilyName | **Toubal** |
| | Particle | |
| | Given Name | **Sara** |
| | Suffix | |
| | Division | Research Unit: Materials, Processes and Environment, Faculty of Technology |
| | Organization | M'hamed Bougara University -Boumerdes |
| | Address | 35000, Boumerdes, Algeria |
| | Phone | |
| | Fax | |
| | Email | |
| | URL | |
| | ORCID | |
| Author | FamilyName | **Aribi** |
| | Particle | |
| | Given Name | **Chouaib** |
| | Suffix | |
| | Division | Research Unit: Materials, Processes and Environment, Faculty of Technology |
| | Organization | M'hamed Bougara University -Boumerdes |
| | Address | 35000, Boumerdes, Algeria |
| | Phone | |
| | Fax | |
| | Email | |
| | URL | |
| | ORCID | |
| Author | FamilyName | **Chentir** |
| | Particle | |
| | Given Name | **Imen** |
| | Suffix | |
| | Division | Research Unit: Materials, Processes and Environment, Faculty of Technology |
| | Organization | M'hamed Bougara University -Boumerdes |
| | Address | 35000, Boumerdes, Algeria |
| | Division | Food Laboratory |
| | Organization | High School of Food Sciences and Agrifood Industries |
| | Address | 16200, Algiers, Algeria |
| | Phone | |
| | Fax | |
| | Email | |
| | URL | |
| | ORCID | |

| | | |
|---|---|---|
| Author | FamilyName | **Bouaissi** |
| | Particle | |
| | Given Name | **Aissa** |
| | Suffix | |
| | Division | |
| | Organization | UNA Developments Ltd, RGC Technology |
| | Address | Plymouth, PL6 7PP, UK |
| | Phone | |
| | Fax | |
| | Email | |
| | URL | |
| | ORCID | |
| Author | FamilyName | **Saidi** |
| | Particle | |
| | Given Name | **Mohammed** |
| | Suffix | |
| | Division | Research Unit: Materials, Processes and Environment, Faculty of Technology |
| | Organization | M'hamed Bougara University -Boumerdes |
| | Address | 35000, Boumerdes, Algeria |
| | Phone | |
| | Fax | |
| | Email | |
| | URL | |
| | ORCID | |



| | | |
|---|---|---|
| Schedule | Received | 2 Jun 2024 |
| | Revised | |
| | Accepted | 9 Jan 2025 |



| | |
|---|---|
| Abstract | The demand for eco-friendly alternatives to petrochemical-based phenolic resins has risen due to increasing concerns about climate change, environmental impact, and manufacturing costs. This study introduces a sustainable approach by partially replacing phenol with lignin, a natural polymer rich in phenolic groups, extracted from Alfa stems. Using the alkaline method, 50% of phenol was substituted with lignin to synthesize phenol–formaldehyde (PF) resins. The synthesized lignin–phenol–formaldehyde (LPF) resin was characterized to verify its chemical structure and physical properties. The resin demonstrated significant antioxidant and antibacterial activity, particularly against *E. coli* and *P. aeruginosa* gram-negative bacteria at a concentration of 20 mg/ml. Additionally, the lignin substitution provided notable advantages over conventional industrial resin formulations. The lignin's properties closely influenced the formulation of the LPF resin, making it similar to the reference CPF resin. However, the lower intensity observed in the LPF resin suggests potential limitations in the methylol group formation compared to the CPF resin. The antioxidant activity of LPF resin has been effectiveness in preventing corrosion on steel surfaces. When applied as an anti-corrosion coating and compared to industrially used CPF resins, LPF resin demonstrates its efficacy in such applications. Also, it should be noted that the impedance modulus of the elaborated resin coating remained consistently low throughout the entire immersion period, indicating its stable performance. |



| | |
|---|---|
| Keywords (separated by '-') | Lignin - Alfa stem - Phenol–formaldehyde resin - Physicochemical characterization - Biological activities - Anticorrosive coatings |
| Footnote Information | |

Proceedings of the Indian National Science Academy
https://doi.org/10.1007/s43538-025-00388-0

RESEARCH PAPER

# Synthesis of resin from Alfa stem to applied as an adhesive corrosion-resistant coating

Sara Toubal[1] · Chouaib Aribi[1] · Imen Chentir[1,2] · Brahim Safi[1] · Aissa Bouaissi[3] · Mohammed Saidi[1]

Received: 2 June 2024 / Accepted: 9 January 2025


## Abstract

The demand for eco-friendly alternatives to petrochemical-based phenolic resins has risen due to increasing concerns about climate change, environmental impact, and manufacturing costs. This study introduces a sustainable approach by partially replacing phenol with lignin, a natural polymer rich in phenolic groups, extracted from Alfa stems. Using the alkaline method, 50% of phenol was substituted with lignin to synthesize phenol–formaldehyde (PF) resins. The synthesized lignin–phenol–formaldehyde (LPF) resin was characterized to verify its chemical structure and physical properties. The resin demonstrated significant antioxidant and antibacterial activity, particularly against *E. coli* and *P. aeruginosa* gram-negative bacteria at a concentration of 20 mg/ml. Additionally, the lignin substitution provided notable advantages over conventional industrial resin formulations. The lignin's properties closely influenced the formulation of the LPF resin, making it similar to the reference CPF resin. However, the lower intensity observed in the LPF resin suggests potential limitations in the methylol group formation compared to the CPF resin. The antioxidant activity of LPF resin has been effectiveness in preventing corrosion on steel surfaces. When applied as an anti-corrosion coating and compared to industrially used CPF resins, LPF resin demonstrates its efficacy in such applications. Also, it should be noted that the impedance modulus of the elaborated resin coating remained consistently low throughout the entire immersion period, indicating its stable performance.

**Keywords** Lignin · Alfa stem · Phenol–formaldehyde resin · Physicochemical characterization · Biological activities · Anticorrosive coatings

## Introduction

With the urgent need to meet net-zero targets, addressing climate change and safeguarding the environment have become top priorities for researchers. The petrochemical industry, involved in producing phenolic products, is experiencing a notable increase in demand across diverse sectors such as dyes, synthetic floor coatings, additives, thermosetting resins, dispersing agents, and paints. There is great promise in utilizing renewable resources, fueled by the presence of plentiful and eco-friendly sources of cellulose and lignin (Tribot et al. 2019). These resources, collectively referred to as lignocellulosic materials, encompass jute, hemp, cotton, Alfa stalk, and wood pulp, boasting lignin levels ranging from 10 to 25% (Hu et al. 2011; Kuhad and Singh 2007). Lignin, in its natural form, not only supports the structural integrity of trees but also acts as a defense mechanism against various chemical and biological threats (Pan et al. 2006). Particularly in plants with sturdy stems like Alfa, lignin plays a pivotal role in providing antimicrobial properties (Qin et al. 2023; Tian et al. 2018), with these characteristics greatly influenced by the source and method of extraction.

Because of these characteristics, lignin demonstrates water insolubility, natural stability, and acts as a binding agent that links cellulose and hemicellulose together. It possesses a three-dimensional macromolecular structure, formed through the random polycondensation and enzymatic dehydrogenation of three alcohol-based monomers. These monomers, distinguished by the number of methoxyl

✉ Brahim Safi
safi_b73@univ-boumerdes.dz

[1] Research Unit: Materials, Processes and Environment, Faculty of Technology, M'hamed Bougara University -Boumerdes, 35000 Boumerdes, Algeria

[2] Food Laboratory, High School of Food Sciences and Agrifood Industries, 16200 Algiers, Algeria

[3] UNA Developments Ltd, RGC Technology, Plymouth PL6 7PP, UK

(OCH3) groups present on the aromatic ring, include p-coumaryl alcohols lacking methoxyl groups, coniferyl alcohols with a single group, and sinapyl alcohols carrying two methoxyl groups (refer to Fig. 1). These three monomers respectively contribute to the formation of H (Hydroxyphenyls), G (Guaiacyls), and S (Syringyls) units within the lignin structure, with the proportion of each unit determined by the biosource (Joe et al. 2023). However, the percentage of p-coumaryl alcohol is typically lower than the others (Dong et al. 2011) (refer to Fig. 1).

The stochastic arrangement of lignin leads to the presence of numerous functional groups (Kaur et al. 2017; Vanholme et al. 2010), which clarifies its chemical compositions and structural configuration (Monteil-Rivera et al. 2013). Lignin molecules are mainly abundant in phenolic hydroxyl (OH) groups, which then undergo reactions with formaldehyde from the phenylpropane unit to produce phenolic resin (Lee et al. 2009; Barton 1988).

Extensive research has focused on producing phenolic resin from agricultural lignin (Zakzeski et al. 2010; Jin Huang et al. 2019). However, a significant hurdle arises from the lower reactivity of lignin or bio-phenols, largely due to the scarcity of extra active sites with formaldehyde needed for synthesizing phenolic-formaldehyde resins (PF) (Sarkar and Adhikari 2000). This challenge elucidates why partial substitution of phenol, usually around 50%, has been proposed. Yet, escalating the substitution rate might detrimentally impact the performance of the end product, especially in certain applications like the wood industry (Ghorbani et al. 2016).

Research has shown that the characteristics of lignin are largely shaped by the extraction method utilized, encompassing various techniques such as alkaline lignin, organosolv, steam exploded lignin, Kraft lignin, and lignosulfonates, with the latter containing notable amounts of sulfur (Caoxing Huang et al. 2022; Effendi et al. 2008). Consequently, extraction methods are divided into two categories (Pilato 2010). The first category involves sulfur-free extraction methods, which include different processes. One commonly employed method is organosolv, which entails extracting lignin from biomass using organic solvents and water at temperatures ranging from 150 to 200 °C (Kuhad and Singh 2007). Solvents such as ethanol, methanol, acetone, ethylene glycol, and organic acids are utilized in this process. Organosolv extraction is widely favored due to its positive environmental impact (Hu et al. 2011; Monteil-Rivera et al. 2013; Saake and Lehnen 2007; Baumberger et al. 2007).

The second category comprises extraction methods involving sulfur, known as lignin soda, which contributes to around 5% of global lignin production (Laurichesse and Avérous 2014). This extraction method primarily involves the hydrolytic cleavage of native lignin using sodium hydroxide solution (NaOH) at temperatures ranging from 150 to 170 °C. However, lignin produced through this method is relatively less chemically modified compared to other types of lignin (Pilato 2010).

In industry, sulfur extraction processes rely on sulfur implementation through two distinct methods. The first method, termed Kraft lignin, entails treating black liquor (Decoction) from the paper industry, where lignin precipitates during the acidification process in the presence of methoxyl and carboxyl groups (Ragauskas, et al. 2014). The second method, known as lignosulfonates or the sulfite process, involves utilizing an aqueous solution of sulfur dioxide ($SO_2$) along with other base solutions such as calcium, sodium, magnesium, and ammonium (Pilato 2010).

The primary objective of this study is to explore a novel approach that uses lignin, which is rich in phenolic groups, as a partial substitute for phenol in the synthesis of phenol–formaldehyde (PF) resins. In this study, 50% of phenol was replaced with lignin, which was extracted using the alkaline method from renewable natural

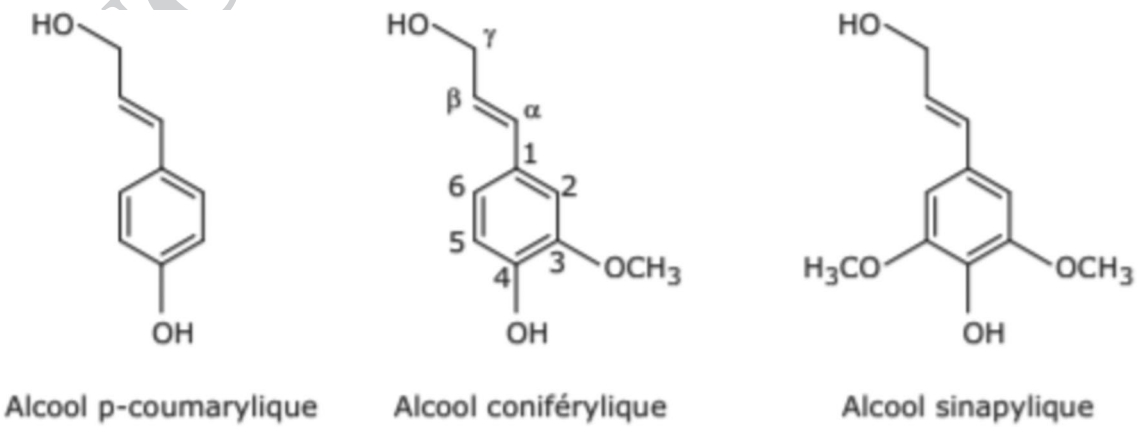


**Fig. 1** Monomers of lignin





Journal : Large 43538 | Article No : 388 | Pages : 17 | MS Code : 388 | Dispatch : 21-1-2025

resources—specifically, raw Alfa stems. The choice of 50% substitution is based on previous research demonstrating that higher substitution rates can adversely affect the resin's mechanical properties, while a 50% replacement offers an optimal balance between sustainability and maintaining desired resin performance. Characterization analyses were carried out to verify the chemical structure and physical properties of the resin with this level of lignin substitution. Additionally, the antioxidant and antibacterial activities of the resulting resin were evaluated.

# Experimental study

## Materials and methods

### Materials

The fiber from esparto plants, sourced from the East region of Algeria, served as the raw material for lignin extraction. Various chemicals were utilized during the extraction and synthesis processes, including Phenol (99%), Formaldehyde solution (37%), Methanol (99%), Sulfuric acid (98%), and Sodium hydroxide (97%). These procedures followed the alkaline method and were consistent with established protocols for lignin extraction and resin synthesis as referenced in the literature (Zakzeski et al. 2010; Jin Huang et al. 2019; Calvo-Flores and Dobado 2010; Toledano et al. 2010; Brunow et al. 1999; Khan et al. 2004a; Lee et al. 2012). To assess the antioxidant activity of lignin, tests were conducted using Dimethyl sulfoxide (DMSO), ABTS radical (2,2′-azino-bis-(3-ethylbenzothiazoline-6-sulfonic acid)), and DPPH radical-scavenging activity. The antibacterial activity of lignin was evaluated using Gram-negative bacteria Escherichia coli and Pseudomonas Sp, as well as Gram-positive Bacteria Staphylococcus aureus.

### Extraction of lignin

The Alfa threads (stems) were washed with distilled water and subsequently dried in an oven at a temperature of $40 \pm 2$ °C for 24 h. The drying process was halted when the difference in weight was quasi-stable, indicating no further change had occurred. During this stage, scanning electron microscopy (SEM) was conducted to gain insight into the morphological structure of the Alfa thread specimens. The SEM analysis revealed a non-homogeneous porous structure, as illustrated in Fig. 2.

The dried stems were fragmented into pieces measuring 3 to 5 cm in length and then mechanically crushed. Subsequently, 40 g of the crushed esparto fiber and 400 g of sodium hydroxide (NaOH) solution with a concentration of 5 mol/l were added to a flask with two open extremities, equipped with a cooling system and a thermometer. The mixture was heated at $100 \pm 2$ °C for 7 h. It has been reported in the literature that this process is more effective for enhancing the antioxidant activity of alkaline lignin (Hussin et al. 2013).

Thereafter, the contents were filtered to the suspended pulp fibers, and neutralized with a 50% solution of sulfuric acid ($H_2SO_4$) under a constant stirring for 7 h. At the end of this stage, lignin precipitates were obtained. These precipitates were recovered via vacuum filtration using filter paper. Subsequently, the resulting mixture was washed with hot distilled water to ensure the removal of any residual sulfuric acid. Finally, the lignin cake obtained was dried in an oven at $40 \pm 2$ °C.

### Synthesis of lignin–phenol–formaldehyde resin

The lignin–phenol–formaldehyde (LPF) resin was prepared in two steps: first, the preparation of lignin-phenol (LP), followed by the polymerization step to produce LPF resin.

In the first step, 85 g of lignin cakes were added to a beaker containing 28 g of phenol. The mixture was then stirred mechanically for 1 h at a temperature of $40 \pm 2$ °C



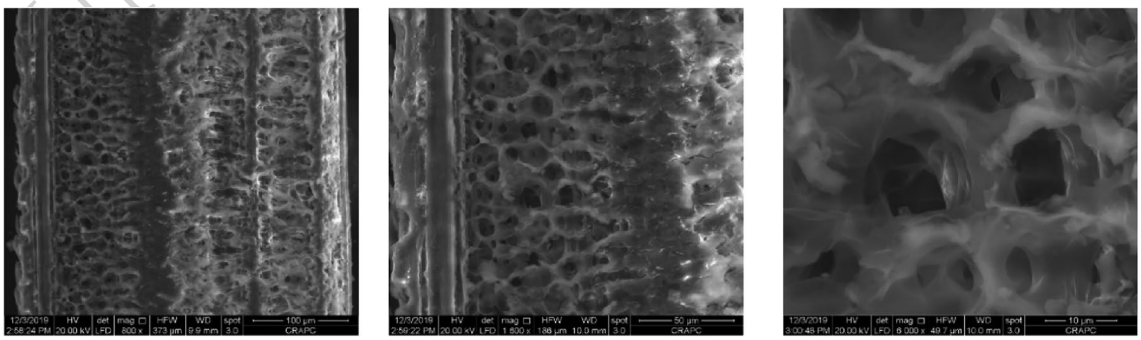

**Fig. 2** Morphology of the Alfa stem

to obtain a homogeneous mass. For the second step, 75 g of LP was mixed with 65.25 g of formaldehyde solution, 30 g of methanol, and 30 ml of distilled water in a four-necked round-bottomed flask equipped with a stirrer, thermometer, reflux condenser, and dropping funnel. The mixture was heated to 80 ± 2 °C using a magnetic stirrer. Subsequently, 3.48 g of NaOH solution, serving as an alkaline catalyst, was slowly added to the mixture over a period of 15 min. The final mixture was left to react for 4 h before cooling to room temperature. The resulting lignin-phenol–formaldehyde resin was then collected.

## Characterization of lignin and the formulated resin

### FTIR analysis

A Fourier transform infrared spectrophotometer (FTIR) was used to identify the synthesized lignin and resin. The analysis was conducted using an iS-10 Thermo Nicolet apparatus operating in ATR mode (attenuated total reflection) with a ZnSe crystal (Serial Number: AKX1501953).

To ensure proper contact between the sample and the crystal, a controlled pressure clamping system was employed. The interface was operated using Omnic 9 processing and analysis software.

### NMR analysis

The chemical structures of lignin and resins were characterized using liquid nuclear magnetic resonance (NMR) spectroscopy in a dimethyl sulfoxide (DMSO) environment. The DMSO solution contained 0.3% tetramethyl silane (TMS) as an internal standard, and the measurements were conducted at a room temperature of 20 ± 2°C. The NMR analysis was performed using Bruker liquid NMR equipment operating at frequencies ranging from 400 to 600 MHz. The equipment was equipped with measuring probes capable of analyzing phenol-glucose organic compounds.

### Thermal analysis

Differential Scanning Thermal Analysis (DSC) and Thermogravimetric Analysis (TGA) were conducted simultaneously using the NETZSCH STA 409PC/PG instrument (Simultaneous Thermal Analysis, Serial Number: 227 2 097 H). This instrument operates based on the differential measurement of thermal effects using two thermoelectric stacks and the measurement of temperature-dependent mass loss. The analyses were carried out under a nitrogen atmosphere, with a heating regime up to 500°C at a rate of 10°C/min.

## Biological activities of lignin extract

**Antioxidant activity** The ABTS + scavenging activity of the lignin extract was assessed following the method outlined by Re, Roberta, et al. (Li et al. 2018). Lignin solutions ranging from 0.25 to 3 mg/ml were prepared for the analysis. The absorbance of these solutions was measured at 734 nm. The chelating activity percentage was calculated using the following formula

$$ABTS^{+}scavening\ activity(\%) = \left[\frac{OD_C + OD_B + OD_S}{OD_C}\right] \times 100. \quad (1)$$

where: ODC, ODB, and ODS represent the absorbances of the control, the blank, and the sample reaction tubes, respectively. The test was triplicated to ensure the accuracy of the results.

The DPPH radical-scavenging activity of the lignin extract was assessed according to Bersuder's procedure (Arasaretnam and Kirudchayini 2019), with slight modifications. Lignin solutions ranging from 0.25 to 3 mg/ml were prepared for the analysis. The DPPH radical-scavenging activity was calculated using the following formula:

$$DPPHradical - scaveninigactivity(\%) = \left[\frac{A_{control} + A_{blanc} - A_{sample}}{A_{control}}\right] \times 100. \quad (2)$$

where $A_{control}$: is the absorbance of the control -containing all reagents except the sample, $A_{blank}$: is the absorbance of the blank -containing all reagents except the DPPH solution. $A_{sample}$: is the absorbance of the sample with the DPPH solution.

**Antibacterial activity** An antibacterial activity test was conducted on the extracted lignin against three species of bacteria, including both Gram-positive and Gram-negative strains: *S. aureus*, *E. coli*, and *P. aeruginosa*. The antibacterial activity of the lignin solution at a concentration of 20 mg/ml was evaluated using a well-diffusion assay against one Gram-negative strain (Escherichia coli and Pseudomonas Sp) and one Gram-positive strain (Staphylococcus aureus-ATCC 25923) (Jiang et al. 2018).

For the assay, overnight cultures of the tested pathogens were evenly spread on sterile Muller Hinton agar plates. Small holes with a diameter of 6 mm were then made on each plate using a sterile cork-borer. Subsequently, 75 µl of the lignin solution was loaded into each hole, allowing the solution to diffuse for 3 h at 4 °C. After diffusion, the plates were incubated at 37 °C for 18 h. The diameter (in mm) of the growth inhibition zone around each hole was measured in duplicate. The appearance of a clear area





Journal : Large 43538 | Article No : 388 | Pages : 17 | MS Code : 388 | Dispatch : 21-1-2025

below or around the sample was considered indicative of antimicrobial activity.

## Results and discussion

### Chemical analyses of the extracted lignin

#### FT-IR spectroscopy

The identification of functional groups and the characteristic absorption bands of the basic unit's G (guaiacyl), S (syringyl), and H (p-hydroxyphenyl propane) of lignin were successfully determined through FTIR spectral analysis, as presented in Table 1. The FTIR spectra of the esparto lignin are illustrated in Fig. 3.

The differences in absorption frequencies of the lignin are characterized by distinct bands and functional groups formed during the extraction process. Specifically, the band at the 3400 $cm^{-1}$ regions, revealed that there is vibration of hydroxyl groups (O–H) bending. The peak at 2950 $cm^{-1}$ characterizes the C–H vibration of the methylene groups and the region of 1500, 1550, and 1610 $cm^{-1}$, shows bands attributed to the aromatic vibrations of the backbone. The band at 1450 $cm^{-1}$ is attributed to the COH deformation in the –CH3 of a methoxyl group, the broad bands at around 1120 $cm^{-1}$, and 1030 $cm^{-1}$ can be ascribed to the presence of the set G units. Furthermore, the band at 830 $cm^{-1}$ could reveal to the presence of the H unit, indicating that the backbone of this lignin contains all three basic units H, G, and S.

#### 1H and 13C NMR spectra of Alfa lignin

The signals ranging between 0.8 and 0.9 ppm are associated with the aliphatic proton fraction in the lignin. The peak at 1.25 ppm indicated in Fig. 4, signifies the presence of hydrogen in the aliphatic group of the lignin (Kalami et al. 2017). The peak around 1.57 ppm is attributed to hydrogen from H2O in the solvent. Therefore, a series of signals ranging from 2.04 to 2.37 ppm are attributed to hydrogen in the –CH groups from aromatic and aliphatic acetylation derivatives (Tejado et al. 2007). The peak at 2.62 ppm can present the DMSO, which was used as a solvent. Additionally, peaks between 3.63 and 3.98 ppm indicate hydrogen in the methoxyl group (–OCH3), which is primarily associated with the G/S ratio (Khan et al. 2004b). This analysis clarifies that the FTIR peak at 1034 $cm^{-1}$ corresponds to a higher G-unit content compared to the peaks 6.84, 6.82, and 5.35ppm, which are attributed to the aromatic protons of guaiacol (G) and syringyl (S) units in the lignin (Laurichesse and Avérous 2014; Vlietinck and Vanden Berghe 1991). The peak observed around 7.26 ppm corresponds to CDCL3 chloroform, which was used as a strong solvent, allowing a large number of samples to be dissolved with a high concentration (Yang et al. 2007).

The identification of carbon in the lignin structure, including aryl ether, aromatic and aliphatic, was performed using C13 NMR (Scholze et al. 2001). Data for the identification of C13 lignin were collected from other works (Glasser and Jain 1993; Zhang et al. 2013). Accordingly, the regions between 107 and 124 ppm correspond to tertiary aromatic carbons, while the range of 58 to 106 ppm represents

**Table 1** Assignments of FTIR spectra of lignin from Alfa stem

| Wave number ($cm^{-1}$) | Assignments | References |
|---|---|---|
| 3400 | Vibration O–H<br>O–H stretching involved in hydrogen bonds | Vanholme et al. (2010), Calvo-Flores and Dobado (2010), Re et al. (1999), Bersuder et al. (1998), Vlietinck and Vanden Berghe (1991), Abdelkefi et al. (2011), Khan et al. (2004b), Serrano et al. (2010) |
| 2950 | C–H elongation vibration in methyl and methylene groups | Calvo-Flores and Dobado (2010), Re et al. (1999), Vlietinck and Vanden Berghe (1991), Abdelkefi et al. (2011), Khan et al. (2004b), Serrano et al. (2010) |
| 1610 | Vibration of the C=O conjugated with the aromatic rings | Calvo-Flores and Dobado (2010), Re et al. (1999), Abdelkefi et al. (2011) |
| 1400, 1500, 1604 | C–C vibrations in the aromatic ring | Re et al. (1999), Vlietinck and Vanden Berghe (1991), Khan et al. (2004b), Serrano et al. (2010) |
| 1123 | Aromatic C–H vibrations related to S units | Vanholme et al. (2010), Brunow et al. (1999), Re et al. (1999), Bersuder et al. (1998) |
| 1034 | Deformation in plan de C–H units of G (if G > S) or/and vibration of C–O bonds in primary alcohols and/or C=O stretching (unconjugated)<br>Vibrations of G units | Vanholme et al. (2010); Brunow et al. (1999), Re et al. (1999), Bersuder et al. (1998), Baumberger et al. (2007), Laurichesse and Avérous (2014) |
| 830 | Vibration of H units | Re et al. (1999) |

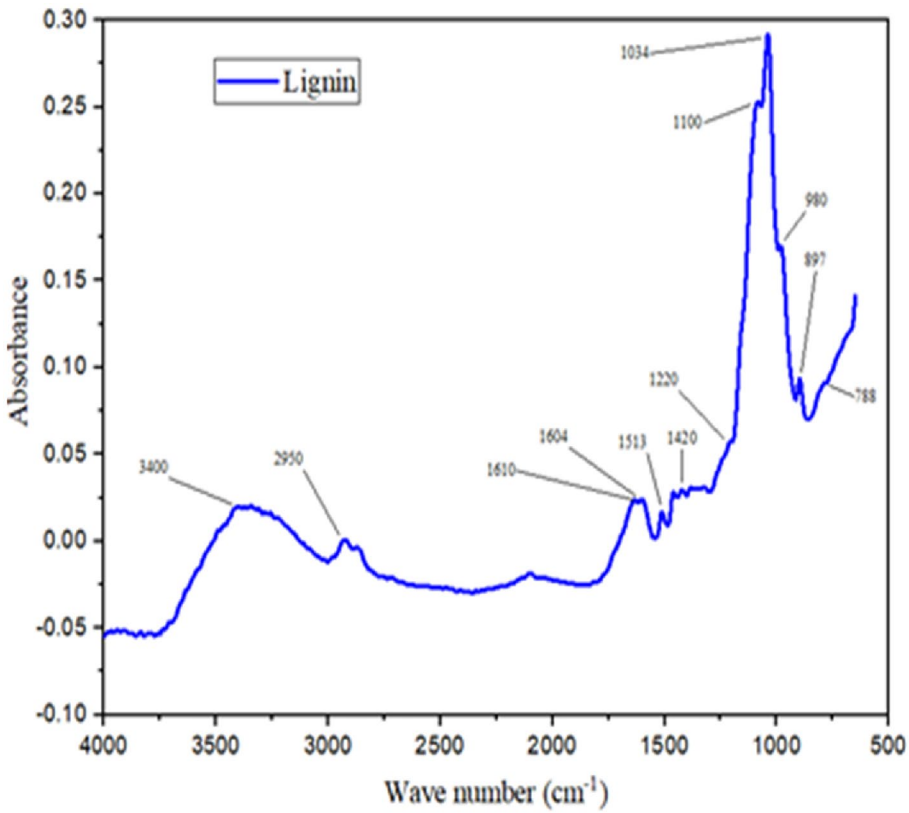


**Fig. 3** FT-IR spectra of lignin extracted from Alfa stem

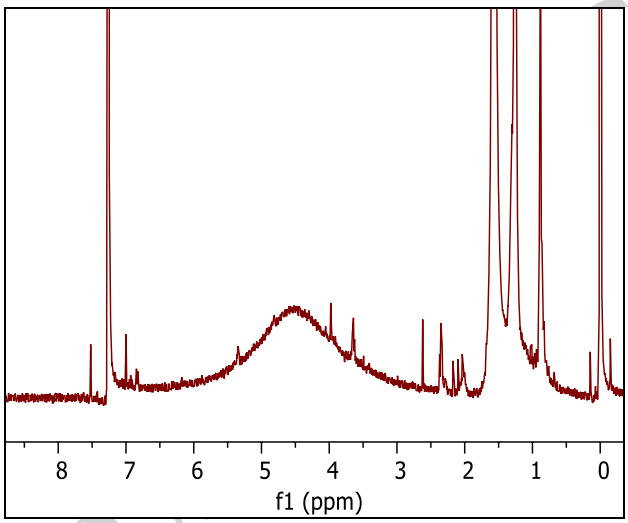


**Fig. 4** 1H NMR spectra of lignin extracted from Alfa stem

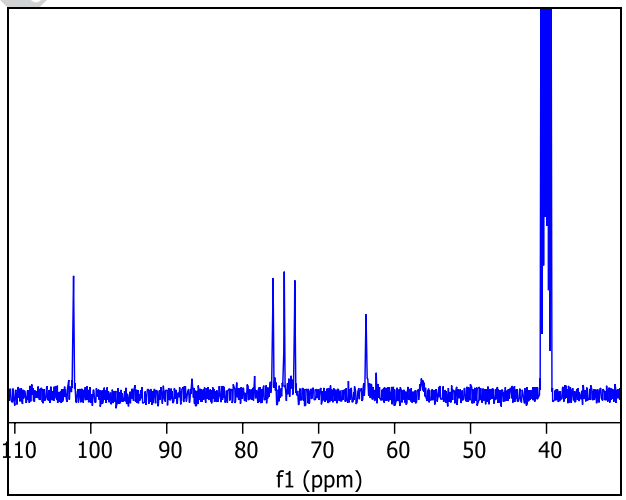


**Fig. 5** C13 NMR spectra of lignin extracted from Alfa stem

oxygenated tertiary aliphatic carbons. The region between 57 and 54.5 ppm is attributed to methoxyl groups attached to the aromatic carbons. The remaining region accounts for non-oxygenated tertiary aliphatic carbons, including B-type carbons in B-5 units and 8-B' units (Kringstad and Mörck 1983).

The C13 NMR spectrum of the esparto lignin, as depicted in Fig. 5, illustrates various carbon resonances. Specifically, the region between 60 and 80 ppm is attributed to oxygenated aliphatic carbons, while the peak at 56 ppm corresponds to the carbon of the methoxyl group (OCH3) in the syringyl and guaiacyl units (Robert et al. 1989). Additionally, the resonance peak observed at 102.5 ppm is associated with aromatic carbons. The low intensity exhibited in this peak suggests that the level of methoxyl groups bound to the aromatic rings of the lignin is low. This limitation can be



Journal : Large 43538 | Article No : 388 | Pages : 17 | MS Code : 388 | Dispatch : 21-1-2025

attributed to several factors, including the consequences of cooking during the lignin extraction process and the potentially low content of guaiacyl (G) and syringyl (S) units, considering that the p-hydroxyphenyl (H) unit is methoxyl-free (Lapierre et al. 1982).

## Thermal characterization of Alfa lignin

### Thermogravimetric analysis (TGA)

Figure 6 illustrates the TGA curve of the extracted lignin, revealing three distinct phases of thermal decomposition. Firstly, a 15% mass loss is observed between room temperature and 100 °C, attributed to the evaporation of absorbed water. Secondly, a mass loss of 33.48% occurs between 200 and 350 °C, primarily due to the degradation of carbohydrate components within the lignin. During this phase, these components are converted into volatile gases such as CO, $CO_2$, and $CH_4$. Finally, a further 40% mass loss is observed within the remaining interval of 350–500 °C. This mass loss is attributed to the degradation of volatile compounds and by-products of the lignin, including phenolic compounds, alcohols, and aldehydic acids.

The TGA curve also depicts heat-initiated degradation processes and decomposition of the lignin structure. It is evident that the thermal properties of lignin depend on its source; however, the degradation process predominantly occurs between 200 and 350 °C. This phase involves the fragmentation of inter-unit bonds and the release of monomers and phenol derivatives into the vapor phase (Serrano et al. 2010; Sjöholm et al. 1992; Thring et al. 1996, 1990; Watkins et al. 2015).

### Differential scanning calorimetry (DSC)

Figure 7 displays an endothermic peak attributed to the removal of moisture when the sample is heated to 100 °C. Additionally, the glass transition temperature is observed at 85.6 °C, characterized by an inflection point in the curve, indicating a higher presence of internal moisture exceeding 20%. The glass transition phase can be attributed to the high molecular weights and purity of the material (Kazayawoko et al. 1992). At temperatures exceeding 200 °C, two distinct exothermic peaks are observed. A small exothermic peak is noted at 304 °C, followed by a larger one at 421.4°C. These peaks are indicative of a carbonization process (Serrano et al. 2010), where the lignin undergoes thermal decomposition leading to the formation of carbonaceous residue.

## Antioxidant and antibacterial activity of lignin

### Antioxidant activity of lignin

The extracted lignin from the Alfa stems exhibits significant chemical properties, primarily attributed to its ability to act as a good proton and electron donor. It demonstrates

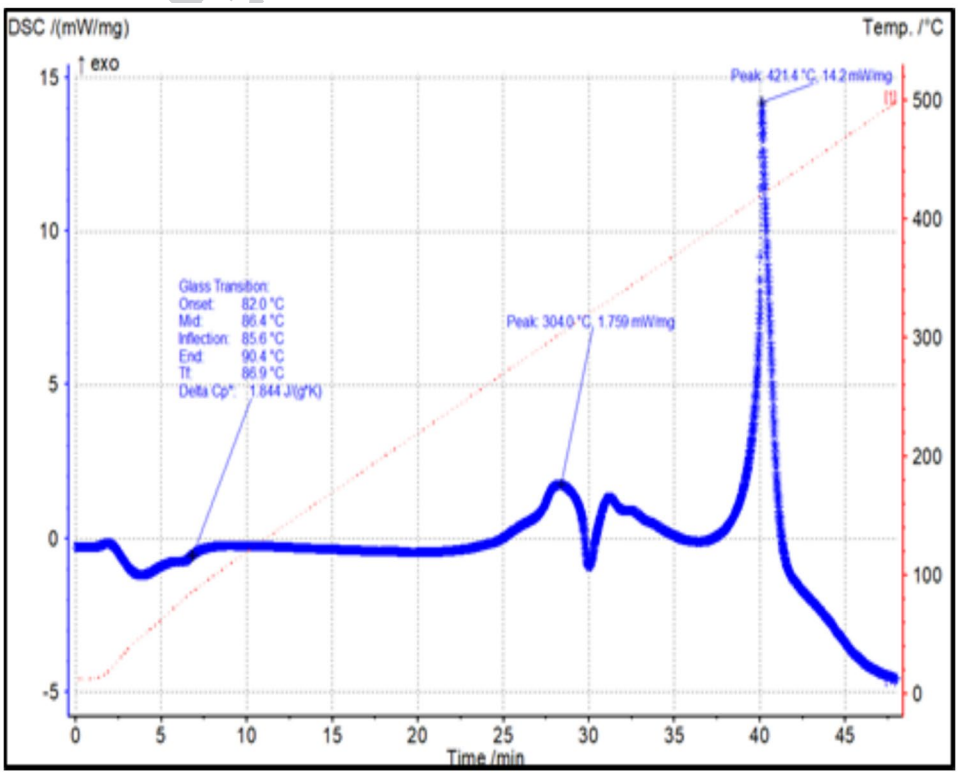


**Fig. 6** TG and DTG of lignin extracted from Alfa stem





Journal : Large 43538 | Article No : 388 | Pages : 17 | MS Code : 388 | Dispatch : 21-1-2025

impressive antioxidant activity, achieving values of 93.9% and 62.7% at a concentration of 3 mg/ml for protons and electrons donation, respectively. This antioxidative capability is indicative of the potential effectiveness of the alkaline oxygen cooking process, which likely promoted oxidation and condensation reactions within the lignin structure, ultimately enhancing its antioxidant activity (Hussin et al. 2013). Moreover, the lignin demonstrates effective antioxidant activity, which can be attributed to the higher content of phenolic hydroxyl groups present within its structure (Matuana et al. 1993; Kim et al. 2017; Penkina et al. 2012). These phenolic hydroxyl groups are known for their ability to scavenge free radicals and inhibit oxidative processes, thereby conferring antioxidative properties to lignin (Tables 2 and 3).

## Antibacterial activity of lignin

Based on the aforementioned antibacterial activity findings, the alpha lignin extract demonstrates effectiveness at a concentration of 20 mg/ml against gram-negative bacteria *E. coli* and *P. aeruginosa*, with inhibition zones of 10.5 mm and 11.5 mm, respectively, as illustrated in Fig. 8. However, no significant effect has been observed when tested against the Gram-positive bacterium S. aureus (with an inhibition zone of 6 mm), which suggests the dependence of antibacterial activity on the type of lignin utilized (Chen and Ho 1995; Zhao et al. 2018), as well as the essential requirement for the presence of phenolic OH groups for antibacterial efficacy (Qin et al. 2023; Sadeghifar et al. 2017). The mechanism of action underlying the antibacterial activity of alpha lignin is effective against gram-negative bacteria such as *E. coli* and *P. aeruginosa*, involving either the attachment of lignin nanoparticles to the cell wall or their penetration into the cell (Zhao et al. 2018; Sadeghifar et al. 2017; Rocca et al. 2018). This effectiveness is primarily attributed to the presence of lipid compounds in the cell walls (Klapiszewski et al. 2015) (Table 4).



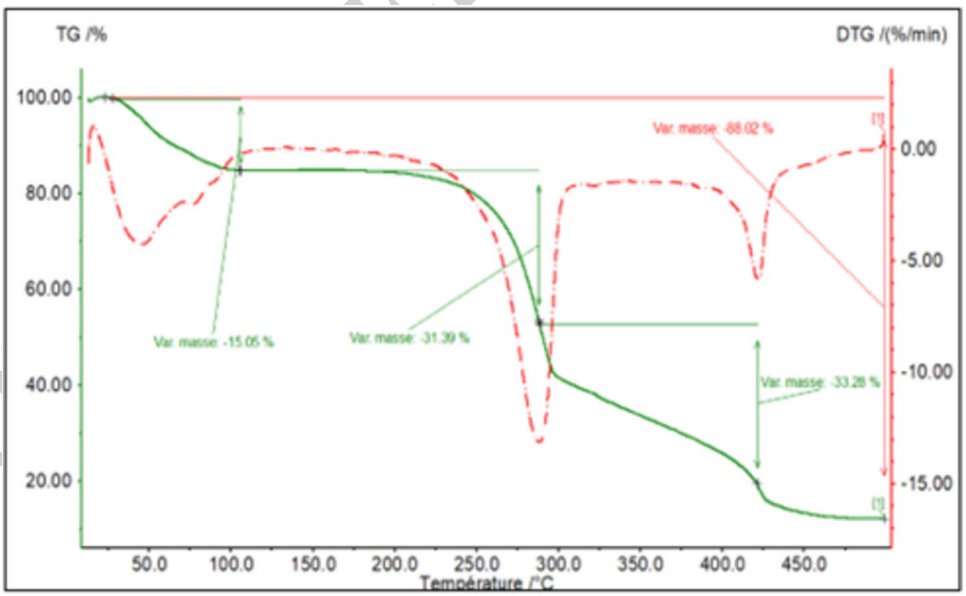


**Fig. 7** DSC calorimetry of lignin extracted from Alfa stem

**Table 2** DPPH radical Value of Alfa lignin

| Lignin concentration (mg/mL) | 0 | 0.25 | 0.5 | 1 | 2 | 3 |
|---|---|---|---|---|---|---|
| Antioxidant activity (%) (medium) | 0 | 17.9 | 32.25 | 57.9 | 86.25 | 93.9 |
| Standard deviation (SD) | 0 | 2.12132 | 0.636396 | 0.707107 | 0.636396 | 0.707107 |

**Table 3** ABTS radical value of alfa lignin

| Concentration lignin (mg/mL) | 0 | 0.25 | 0.5 | 1 | 2 | 3 |
|---|---|---|---|---|---|---|
| Activity antioxidant (%) (Moyenne) | 0 | 8.8 | 16.25 | 30.9 | 46.85 | 62.7 |
| Standard deviation (SD) | 0 | 0.282843 | 0.919239 | 1.697056 | 1.202082 | 0.282843 |



Journal : Large 43538 | Article No : 388 | Pages : 17 | MS Code : 388 | Dispatch : 21-1-2025

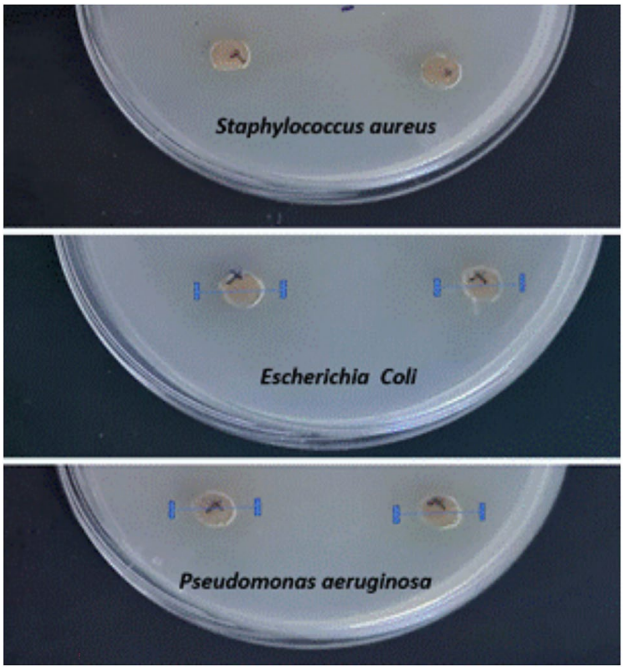


**Fig. 8** Antibacterial activity of Alfa lignin

**Table 4** Alfa lignin value for potential antibacterial activity

| | Inhibition zone (mm) |
|---|---|
| *E. coli* | 10.50 ± 0.71 |
| *S. aureus* | 0.00 ± 00 |
| Pseudo | 11.50 ± 0.71 |

## Characterization of resin

### FTIR analysis

The lignin–phenol–formaldehyde (LPF) resin formulation was analysed using the FTIR technique and compared with the commercial phenol–formaldehyde (CPF) resin, as exhibited in Fig. 9. From the spectra displayed in Fig. 9, both LPF and CPF resins show absorption peaks at 3383 $cm^{-1}$, 3347 $cm^{-1}$, and 3393 $cm^{-1}$, which can be attributed to the presence of OH groups (Bersuder et al. 1998). The frequencies of Phenol were characterized at the peaks 1610 $cm^{-1}$, 1475 $cm^{-1}$, 1240 $cm^{-1}$, 1170 $cm^{-1}$, 1010 $cm^{-1}$, and 785 $cm^{-1}$ (Lee et al. 2009; Vattem et al. 2004; Dong et al. 2012), with peaks at 1662 $cm^{-1}$ and 1610 $cm^{-1}$ could correspond to the vibration of the aromatic ring C=C bonds (Vattem et al. 2004). Notably, the peak at 1240 $cm^{-1}$ observed in the LPF resin spectrum exhibited higher intensity compared to the commercial resin. This observation suggests a greater extent of C–O stretching vibration of the phenolic-OH groups in the LPF resin compared to the commercial resin. This difference could be attributed to the partial replacement of phenol

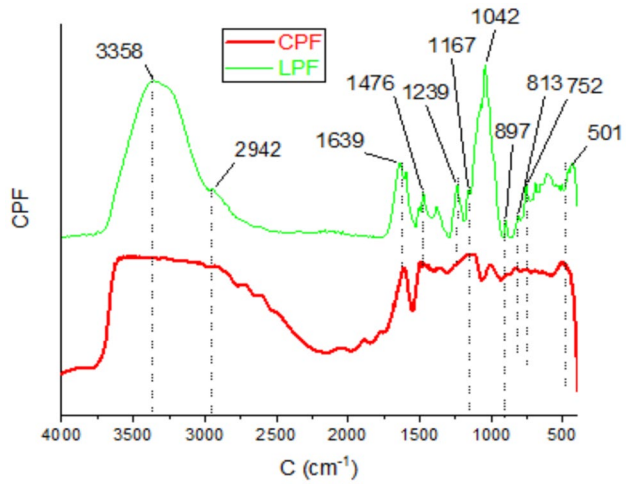


**Fig. 9** FT-IR spectra of CPF and LPF resin

by lignin, which contains both phenolic and non-phenolic units in the LPF resin, thus resulting in a higher concentration of phenolic-OH groups in LPF resins compared to commercial resins (Kalami et al. 2017). The FTIR analysis indicates that the LPF resin shares similar spectra with CPF resins, suggesting that LPF molecules possess a common molecular structure with CPF.

### 1H and 13C NMR spectroscopy of LPF and CPF

The spectra of the 1H aromatic protons of the CPF and LPF resins are depicted in Fig. 10. The qualitative resemblance between the two spectra is evident, indicating a high degree of similarity in their molecular structures, which aligns well with the FTIR results. The primary absorption bands above 6 ppm correspond to the presence of aromatic protons (Bedmutha et al. 2011). Bands observed between 4.6 and 4.5 ppm suggest the presence of methylene protons from the hydroxymethyl groups adjacent to the aromatic rings, while bands ranging from 3.9 to 2.6 ppm indicate methoxylated protons, and those between 3.27 and 3.12 ppm signify methylene protons of the hydroxyl groups. Additionally, bands in the range of 3.3 to 3.27 ppm represent the hydroxyl protons. Specifically, in the LPF spectrum, aromatic acetate protons are located between 2.2 and 2.6 ppm, whereas in the CPF spectrum, aliphatic protons are observed with absorbance between 1.5 and 0.8 ppm (Khan et al. 2004b; Serrano et al. 2010; Kalami et al. 2017; Tejado et al. 2007; Yang et al. 2007; Scholze et al. 2001; Glasser and Jain 1993; Zhang et al. 2013; Kringstad and Mörck 1983; Robert et al. 1989; Lapierre et al. 1982; Sjöholm et al. 1992; Thring et al. 1996, 1990; Watkins et al. 2015; Kazayawoko et al. 1992; Matuana et al. 1993; Kim et al. 2017; Penkina et al. 2012; Chen and Ho 1995; Zhao et al. 2018; Sadeghifar et al. 2017; Rocca et al. 2018; Klapiszewski et al. 2015; Vattem et al. 2004;

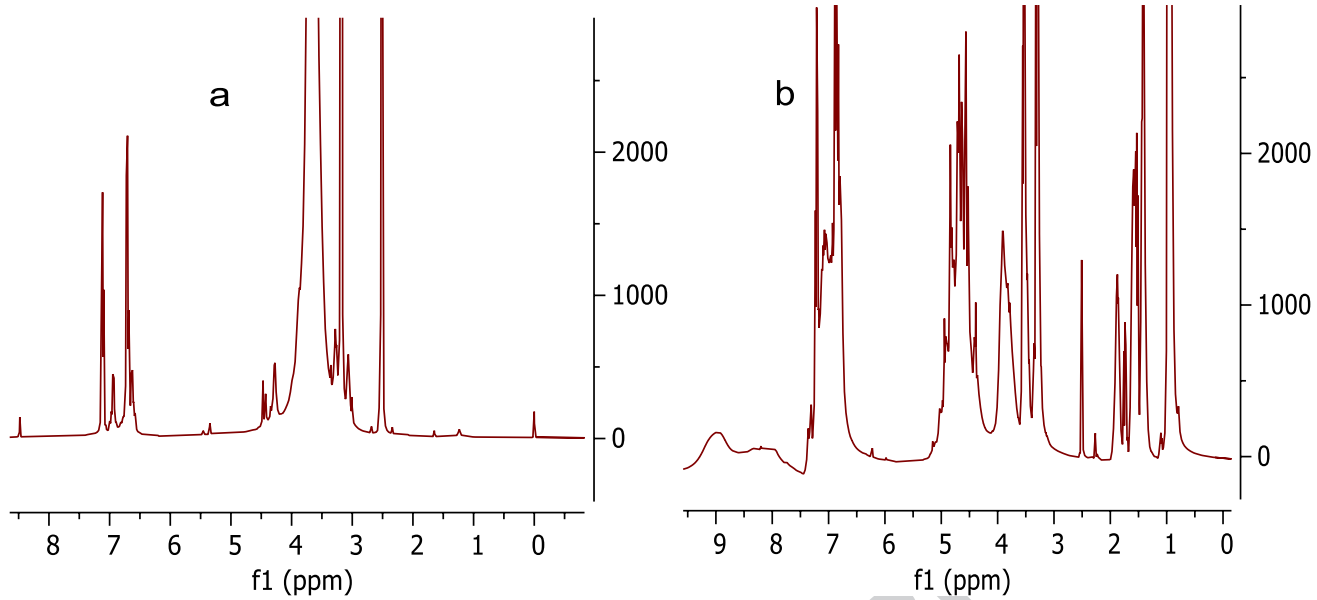


**Fig. 10** 1H spectra of: **a** LPF, **b** CPF

Dong et al. 2012; Bedmutha et al. 2011; Poljansek and Krajnc 2005).

Solvent peaks are discernible at points corresponding to 2.37, 2.51, and 2.30 ppm. The spectral differences in the LPF resin, including those associated with methanol binding, are explained by its formation during the synthesis process. Additionally, the presence of methylene bridges and other functional groups in the lignin structure plays a key role in influencing the resin's properties. The higher intensity of specific peaks in the CPF resin suggests a greater concentration of methoxyl groups attached to aromatic rings compared to the LPF resin. These variations in peak intensities and chemical shifts reflect differences in the molecular structures of LPF and CPF resins, which in turn affect their thermal stability, mechanical properties, and suitability for various applications. In conclusion, while both resins share a similar structural foundation, the substitution of phenol with lignin alters specific key properties. This modification must be considered when evaluating their performance as adhesive materials.

The C13 NMR spectra of LPF and CPF phenolic resins show chemical shifts between 39 and 40.57 ppm, indicative of the presence of methylene bridges. Additionally, this characteristic can also be observed in the range of 34.75–34.85 ppm for CPF resin (Li et al. 2016). Notably, the LPF resin exhibits a chemical shift of 49.07 ppm attributed to the presence of methanol formed during the synthesis process of the phenolic resin (McElroy and Lai 1988; Alonso et al. 2001).

In Fig. 11, the methyl groups exhibit displacements between 61.52 and 61.64 ppm for the CPF resin, and at 60.35 and 63.70 ppm for the LPF resin. Additionally, in the LPF resin, a displacement is observed at 94 ppm, indicating the presence of dimethylene ether bridges. This observation corroborates the condensation process that occurred between two methyl groups during the preparation of this resin. Furthermore, a displacement at 102.21 ppm is evident in the LPF resin, corresponding to ortho-substituted carbons, which contrasts with the CPF resin, where no displacement is observed between 69.0 and 74.0 ppm (Rego et al. 2004). The unsubstituted ortho-carbons are detected at 115.45, 115.38, 115.33, 115.20, 115.13, and 115.07 ppm for the CPF resin, while in the LPF resin, they are observed only at 118.27, 116.08, 115.99, 115.73, and 115.54 ppm with a lower intensity. This decrease can be attributed to the substitution of lignin, as the content of reactive sites of lignin is lower than that of phenol. This is further supported by the exclusive displacement in CPF of the unsubstituted para-carbon of the aromatic ring at 119.17, 119.12, and 119.07 ppm.

A notable displacement between 126.68 and 131.69 ppm is evident in the CPF resin compared to the displacement in the LPF resin, which falls between 127.25 and 132.08 ppm. This displacement is attributed to ortho and para-substituted carbon sites on the aromatic rings. Specifically, the CPF resin exhibits a distinctive displacement at 132.34 and 132.51 ppm, corresponding to para-substituted carbon sites. However, two shifts at 156.52 and 159.09 ppm are observed in the LPF resin, along with a shift band ranging from 153.45 to 157.05 ppm in the CPF resin, both attributed to phenoxy carbons. This observation confirms the limitation of lignin reactive sites (McElroy and Lai 1988; Yi et al. 2016; Werstler 1986).





Journal : Large 43538 | Article No : 388 | Pages : 17 | MS Code : 388 | Dispatch : 21-1-2025

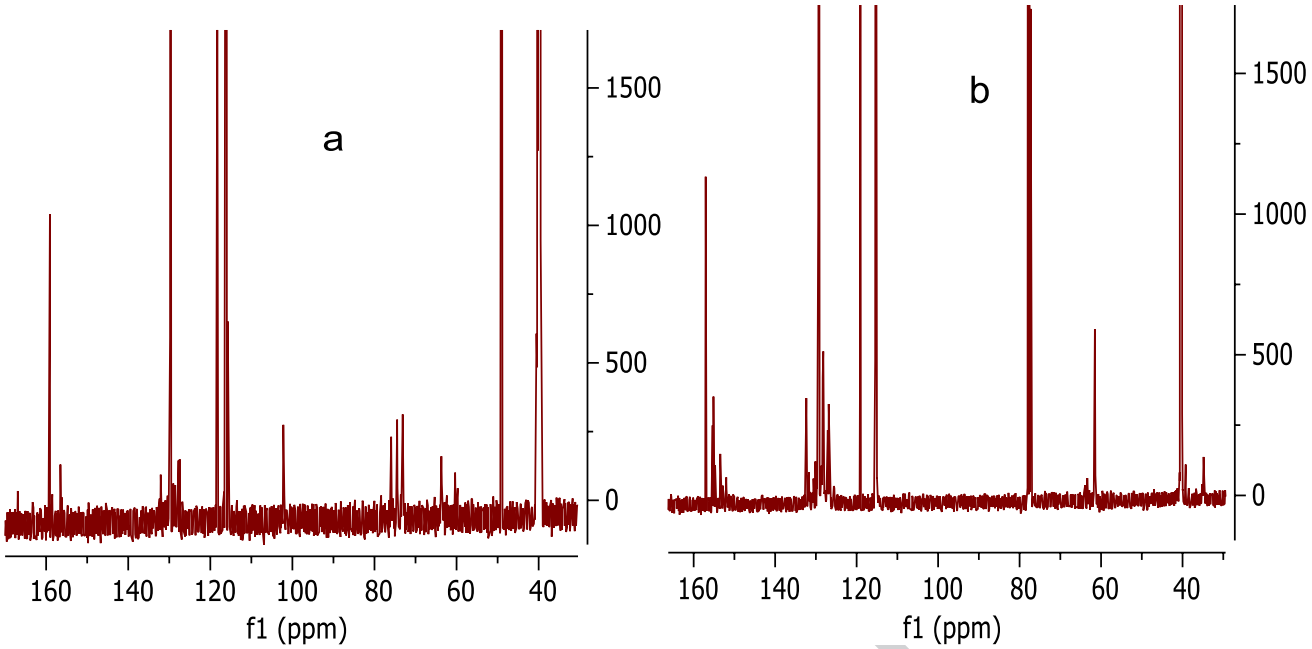


**Fig. 11** C13 spectra of: **a** LPF, **b** CPF

## Thermal analysis DSC–ATG

The TGA curve revealed three distinct decomposition phases for LPF resin: moisture evaporation below 100 °C, carbohydrate decomposition between 200 °C and 350 °C, and volatile compound degradation between 350 °C and 500 °C, the mass change of LPF resin exhibits greater intensity than CPF resin at lower temperatures, typically below 150 °C for LPF and 220 °C for CPF. Beyond these temperatures, the evolution becomes more similar until reaching 400 °C. At this point, the mass change in LPF accelerates, as indicated by the DTG curve. It's noteworthy that the weight loss is higher in LPF compared to CPF resin, confirming findings in the literature which suggest that the incorporation of lignin in the resin formulation decreases the thermal stability of the final product due to its lower molecular weight and cross-linking density of LPF on average, resulting in reduced reactivity (Calvo-Flores and Dobado 2010; Fan et al. 2009; Neiss and Vanderheiden 1994). Consequently, this leads to a lower onset of glass transition, where LPF resin exhibits greater exothermicity above 200 °C. Therefore, the curing temperature for LPF resin is higher than that for CPF resin. Quantitatively, these values may vary depending on factors such as lignin content, source, and extraction method (Trosa and Pizzi 2001).

Differential scanning calorimetry (DSC) is used to identify the glass transition temperature (Tg), which indicates the resin's transition from a brittle to a rubbery state. The results in Figs. 12 and 13 show that LPF resin had a lower Tg than CPF resin, indicating reduced molecular rigidity. This suggests that the incorporation of lignin decreases the resin's cross-linking density, which influences its thermal response and flexibility at different temperatures compared to CPF resin, particularly when exposed to fluctuating environmental conditions. These data suggest that LPF resin, although less thermally stable than CPF, retains sufficient properties to be used in applications requiring moderate thermal resistance.

## Application of elaborated LPF resin in paints

To practically evaluate the synthesized resin, three formulations were prepared using the SOUDAFER BRUN ROUGE solution. These formulations consisted of three types of resins: liquid CPF resin, LPF formulated resin, and CPF* resin (in powder form). The formulations were then applied to metal plate surfaces in two different thicknesses: 100µ for characterization tests and 200µ thickness for corrosion testing. Table 5 presents the results of the characterization tests obtained during the process.

### Electrochemical study

An investigation into the electrode/electrolyte interface, similar to the case of aqueous corrosion, was conducted using electrochemical processes. This process necessitates equipment capable of controlling and measuring electrical potentials and currents at an electrochemical interface (see Fig. 14). The electrochemical cell utilized in this study comprises the following components:

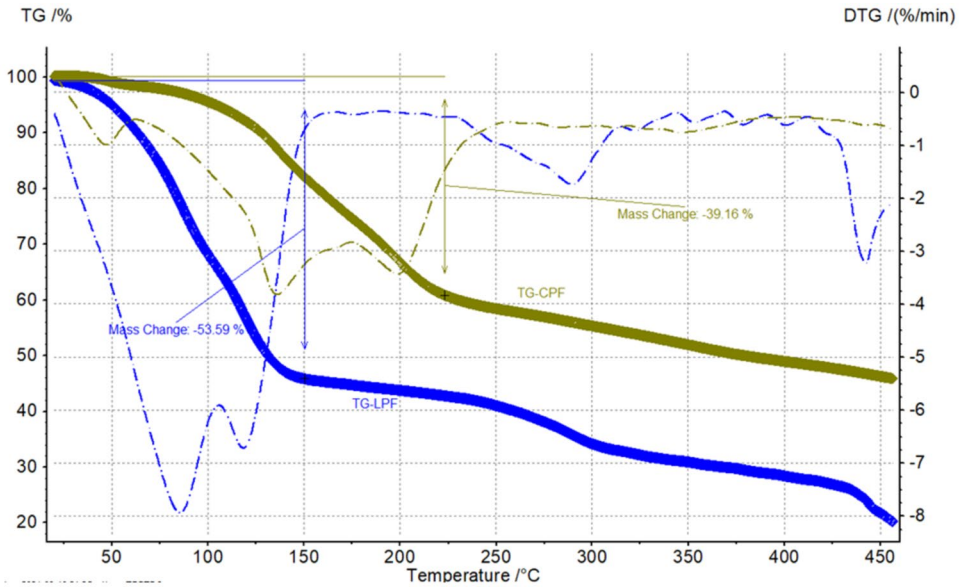


**Fig. 12** TG (**a**) and DTG (**b**) of CPF and LPF resin

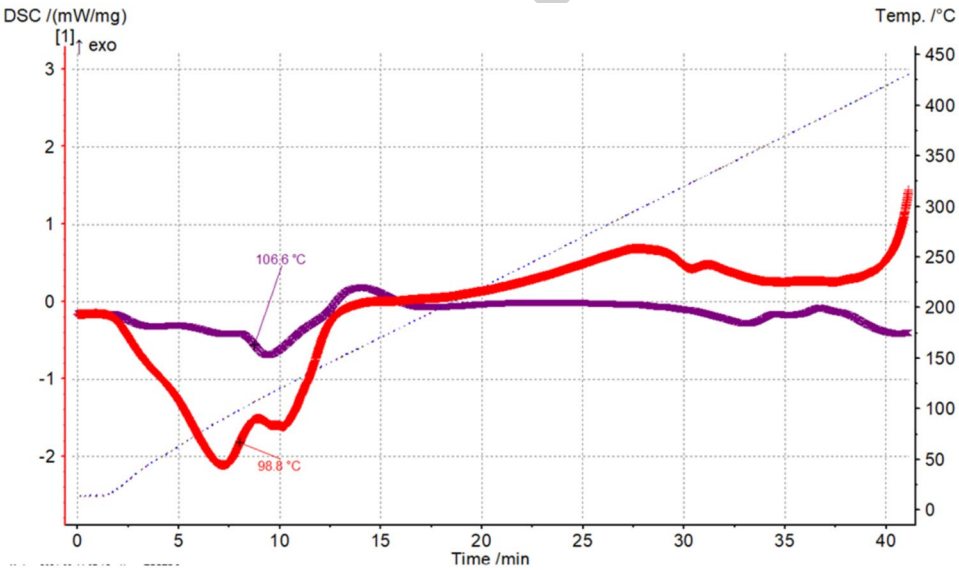


**Fig. 13** DSC calorimetry of CPF and LPF resin

- A PVC tube with a surface area of 15.9 $cm^2$ bonded to a painted steel plate.
- Electrolyte: 70 ml of 3.5% NaCl solution (aerated and at room temperature).
- Immersion time 1 h.
- Three electrodes: (One platinum counter electrode (CE); a saturated calomel reference electrode (RE): Hg/$Hg2Cl_2$(ECS and a working electrode (WC): in which its surface used as a site for the electron transfer reaction.

The interfacial electrical properties were characterized using the electrochemical impedance spectroscopy (EIS) technique. This involves measuring the response of an electrode to a low-amplitude sinusoidal potential perturbation. In this study, impedance measurements were conducted in potentiostatic mode, with a disturbance amplitude of 10 mV and a frequency range from 1 mHz to 100 kHz. Impedance diagrams were obtained using a PARSTAT 4000 Potentiostat/Galvanostat/EIS Analyzer, controlled with VersaStudioTM electrochemistry software.

Figures 15 and 16 show Bode diagrams generated in a 3.5% NaCl solution, covering a frequency range from 10 mHz to 100 kHz, with an amplitude of 10 mV around the open-circuit potential.

The state of coating finish primarily relies on the values of the modulus of low-frequency electrochemical impedance (|Z|0.05), which can be equated to the polarization resistance (as depicted in Fig. 17).



Journal : Large 43538 | Article No : 388 | Pages : 17 | MS Code : 388 | Dispatch : 21-1-2025

**Table 5** Resin characterization results

| Characteristics | Soudafer CPF (Resin Ref.) | Soudafer LPF | Soudafer CPF* |
|---|---|---|---|
| Viscosity (flow time) CF4 cut | 95 s at 28°c | 140 s at 28°c | 120 s at 25°c |
| Wet thickness(µ) | 100 | 100 | 100 |
| Dry thickness (µ) | 15–23 | 15–21 | 15–25 |
| Fineness | 5.5 | 5.5 | 5 |
| Dry extract (%) | 31.42 | 29.74 | 25 |
| Stability | Stable | Stable | Stable |
| Appearance (gloss) (%) | 11 | 0.3 | 14.5 |
| Adhesion | Good | Very good | Bon |
| Stamping (7 mm) | Good | Good | Good |
| Shock | Good | Good | Good |
| Hardness (dry) | 180 '' | 189'' | 94'' |
| Density | 0.971 | 0.976 | 0.980 |
| Bending | Good | Good | Good |

*Powder form



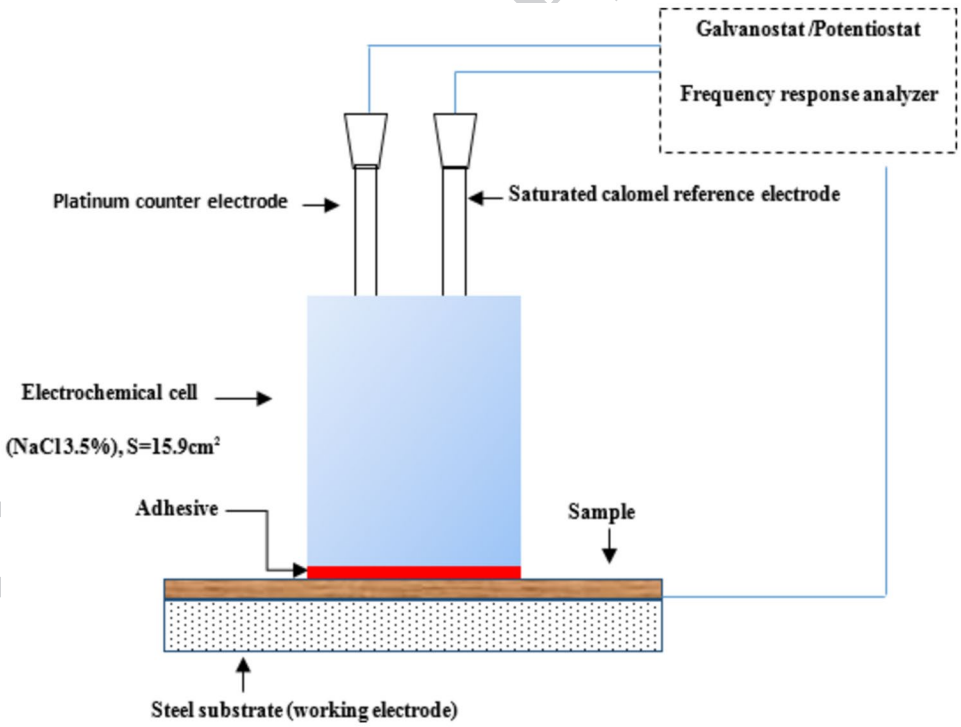


**Fig. 14** Schematic description of the electrochemical cell used

The evolution of Bode plots of healed coatings during the immersion process in 3.5% NaCl solutions for 1 h is also presented in Fig. 15. It has been observed that the impedance modulus of the elaborated resin coating remained consistently low throughout the entire immersion period. From Figs. 16 and 17, it is evident that the coating containing CPF demonstrated a good barrier property after 1 h of immersion in the NaCl solution, with the best impedance modulus observed at the low frequency of 0.1 Hz.

## Conclusion

This study was involves utilizing lignin—abundant in phenolic groups—as a partial substitute for 50% of phenol in the synthesis of phenol-formaldehyde (PF) resins. The obtained LPF resin was utilized as an adhesive corrosion-resistant coating and was compared to other commercially available corrosion coatings to evaluate its performance.

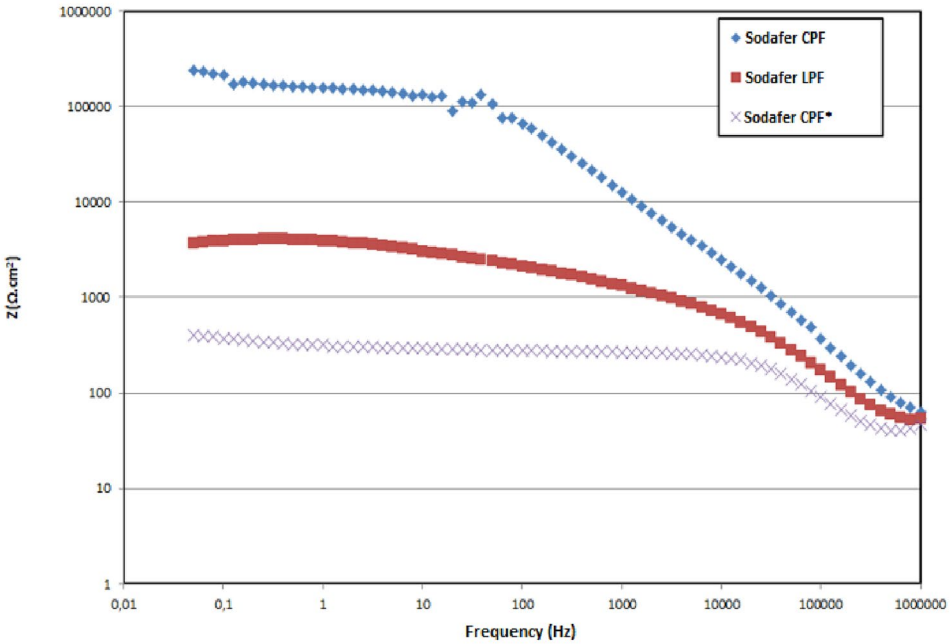


**Fig. 15** Bode plots of impedance versus frequency after 1h immersion in 3.5% NaCl solution

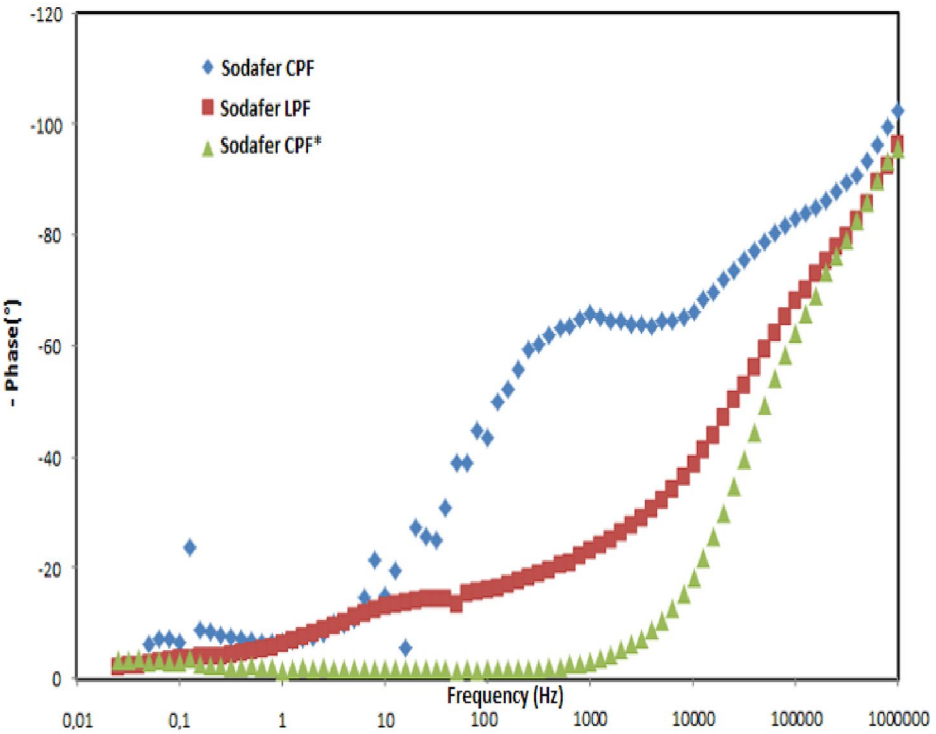


**Fig. 16** Bode plots showing phase versus frequency after 1h immersion in 3.5% NaCl solution

Based on our results, the following conclusions can be drawn:

- The alkaline method employed for the extraction of lignin from the Alfa stem resulted in the production of thermally stable lignin up to 250 °C.
- FTIR and NMR analyses confirmed a low content of methoxyl bound to the aromatic rings of the lignin extracted, with higher G (gaiacyl) unit contents compared to S (syringyl) units.



Journal : Large 43538 | Article No : 388 | Pages : 17 | MS Code : 388 | Dispatch : 21-1-2025

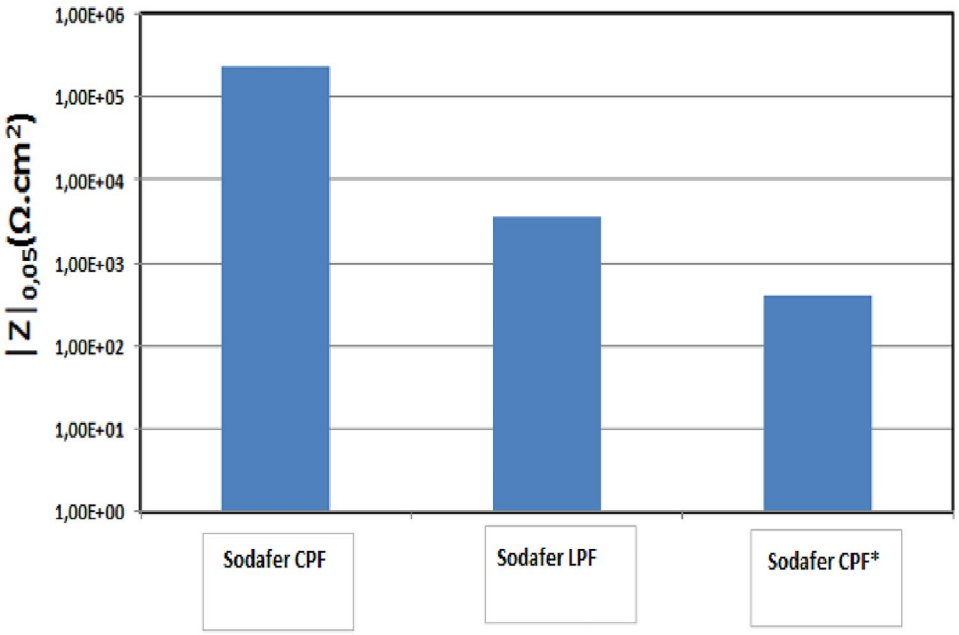


**Fig. 17** The modulus of the low-frequency electrochemical impedance (|Z|0.05)

- Alkaline lignin exhibits potential utility as an antioxidant and antibacterial agent against gram-negative bacteria, attributed to the presence of phenolic OH groups.
- The specifications of the extracted lignin directly influence the properties of the formulated resin (LPF). Structurally, LPF is similar to the reference resin (CPF); however, quantitatively, the low intensity of peaks in the formulated resin suggests limitations in the methylol groups compared to CPF resin.
- The presence of methanol in the LPF phenolic resin during the synthesis process was evidenced by C13 NMR, resulting in decreased thermal stability and increased exothermic release compared to the CPF reference.
- The decomposition mechanism of both resins remains similar. For the application of elaborated resin coatings, it is noteworthy that the coating comprising CPF demonstrated effective barrier properties after 1 h of immersion in a NaCl solution.

**Acknowledgements** The authors express their gratitude for the support from the National Paint Company (ENAP), as well as the Research Unit of Materials, Processes, and Environment (UR-MPE) and the Centre for Physicochemical Research and Analysis (CRAPC).

## References

Abdelkefi, F., Ammar, H., Mlayeh, B., Abid, S., El Gharbi, R.: Caractérisaation de la lignine extraite de l'alfa. J. Soc. Chim. Tunis. **13**, 7–15 (2011)

Alonso, M.V., Rodríguez, J.J., Oliet, M., Rodríguez, F., Garcia, J., Gilarranz, M.A.: Characterization and structural modification of ammonic lignosulfonate by methylolation. J. Appl. Polym. Sci. **82**(11), 2661–2668 (2001)

Arasaretnam, S., Kirudchayini, T.: Studies on synthesis, characterization of modified phenol formaldehyde resin and metal adsorption of modified resin derived from lignin biomass. Emerg. Sci. J. **3**(2), 101–108 (2019)

Barton, F.E., II.: Chemistry of lignocellulose: Methods of analysis and consequences of structure. Anim. Feed Sci. Technol. **21**(2–4), 279–286 (1988)

Baumberger, S., et al.: Molar mass determination of lignins by size-exclusion chromatography: towards standardisation of the method. Holzforschung **61**, 459–468 (2007). https://doi.org/10.1515/HF.2007.074

Bedmutha, R., et al.: Insecticidal and bactericidal characteristics of the bio-oil from the fast pyrolysis of coffee grounds. J. Anal. Appl. Pyrolysis **90**(2), 224–231 (2011)

Bersuder, P., Hole, M., Smith, G.: Antioxidants from a heated histidine-glucose model system. I: investigation of the antioxidant role of histidine and isolation of antioxidants by high-performance liquid chromatography. J. Am. Oil Chem. Soc. **75**(2), 181–187 (1998)

Brunow, G., Lundquist, K., Gellerstedt, G.: Lignin. In: Sjöström, E., Alén, R. (eds.) Analytical Methods in Wood Chemistry Pulping and Papermaking. Springer, Berlin (1999)

Calvo-Flores, F.G., Dobado, J.A.: Lignin as renewable raw material. Chemsuschem **3**(11), 1227–1235 (2010)

Caoxing Huang, Y.D., Peng, Z., Li, J., Li, X., Jiang, X.: Unlocking the role of lignin for preparing the lignin-based wood adhesive: a review. Ind. Crops Prod. (2022). https://doi.org/10.1016/j.indcrop.2022.115388

Chen, C., Ho, C.: Antioxidant properties of polyphenols extracted from green and black teas. J. Food Lipids **2**(1), 35–46 (1995)

Dong, X., Dong, M., Lu, Y., Turley, A., Jin, T., Wu, C.: Antimicrobial and antioxidant activities of lignin from residue of corn stover to ethanol production. Ind. Crops Prod. **34**(3), 1629–1634 (2011)

Effendi, A., Gerhauser, H., Bridgwater, A.V.: Production of renewable phenolic resins by thermochemical conversion of biomass: a review. Renew. Sustain. Energy Rev. **12**(8), 2092–2116 (2008)

Fan, D., Chang, J., Li, J., Mao, A., Zhang, L.: 13C-NMR study on the structure of phenol-urea-formaldehyde resins prepared by methylolureas and phenol. J. Appl. Polym. Sci. **112**(4), 2195–2202 (2009)

Ghorbani, M., et al.: Lignin phenol formaldehyde resoles: the impact of lignin type on adhesive properties. BioResources **11**(3), 6727–6741 (2016)

Glasser, W.G., Jain, R.K.: Lignin derivatives. I. Alkanoates. Holzforschung **47**(3), 225–233 (1993). https://doi.org/10.1515/hfsg.1993.47.3.225

He, G., Yan, N.: Influence of the synthesis conditions on the curing behavior of phenol–urea–formaldehyde resol resins. J. Appl. Polym. Sci. **95**(6), 1368–1375 (2005)

Hu, L., Pan, H., Zhou, Y., Zhang, M.: Methods to improve lignin's reactivity as a phenol substitute and as replacement for other phenolic compounds: a brief review. BioResources **6**(3), 3515–3525 (2011). https://doi.org/10.15376/biores.6.3.hu

Hussin, M.H., Rahim, A.A., Ibrahim, M.N.M., Brosse, N.: Physicochemical characterization of alkaline and ethanol organosolv lignins from oil palm (*Elaeis guineensis*) fronds as phenol substitutes for green material applications. Ind. Crops Prod. **49**, 23–32 (2013)

Jiang, B., Zhang, Y., Gu, L., Wu, W., Zhao, H., Jin, Y.: Structural elucidation and antioxidant activity of lignin isolated from rice straw and alkali-oxygen black liquor. Int. J. Biol. Macromol. **116**, 513–519 (2018)

L. G. Jin Huang, S. Fu, Ed., Chapter 3 - chemical modification of lignin, in Lignin Chemistry and Applications, Elsevier, 2019, pp. 51–78. https://doi.org/10.1016/B978-0-12-813941-7.00003-5.

Joe, M.S., Sudherson, D.P.S., Suyambulingam, I., et al.: Extraction and characterization of novel biomass–based cellulosic plant fiber from *Ficus benjamina* L. stem for a potential polymeric composite reinforcement. Biomass Conv. Bioref. (2023). https://doi.org/10.1007/s13399-023-03759-z

Kalami, S., Arefmanesh, M., Master, E., Nejad, M.: Replacing 100% of phenol in phenolic adhesive formulations with lignin. J. Appl. Polym. Sci. **134**(30), 45124 (2017)

Kaur, R., Uppal, S.K., Sharma, P.: Antioxidant and antibacterial activities of sugarcane bagasse lignin and chemically modified lignins. Sugar Tech **19**, 675–680 (2017)

Kazayawoko, J.-S., Riedl, B., Poliquin, J., Barry, A.O., Matuana, L.M.: A lignin–phenol–formaldehyde binder for particleboard Part 1. Thermal characteristics. Holzforschung **46**(3), 257–262 (1992). https://doi.org/10.1515/hfsg.1992.46.3.257

Khan, M.A., Ashraf, S.M., Malhotra, V.P.: Eucalyptus bark lignin substituted phenol formaldehyde adhesives: a study on optimization of reaction parameters and characterization. J. Appl. Polym. Sci. **92**(6), 3514–3523 (2004a)

Khan, M.A., Ashraf, S.M., Malhotra, V.P.: Development and characterization of a wood adhesive using bagasse lignin. Int. J. Adhes. Adhes. **24**(6), 485–493 (2004b)

Kim, D., et al.: Extraction and characterization of lignin from black liquor and preparation of biomass-based activated carbon therefrom. Carbon Lett. **22**, 81–88 (2017)

Klapiszewski, Ł, et al.: Kraft lignin/silica–AgNPs as a functional material with antibacterial activity. Colloids Surfaces B Biointerfaces **134**, 220–228 (2015)

Kringstad, K.P., Mörck, R.: 13C-NMR spectra of kraft lignins. Holzforschung **37**(5), 237–244 (1983). https://doi.org/10.1515/hfsg.1983.37.5.237

Kuhad, R., Singh, A.: Lignocellulose biotechnology: future prospects. IK International Publishing Hause Pvt Ltd, Kindle Edi (2007)

Kuroe, M., Tsunoda, T., Kawano, Y., Takahashi, A.: Application of lignin-modified phenolic resins to brake friction material. J. Appl. Polym. Sci. **129**(1), 310–315 (2013)

Lapierre, C., Lallemand, J.Y., Monties, B.: Evidence of poplar lignin heterogeneity by combination of 13C and H NMR spectroscopy. Holzforschung **36**(6), 275–282 (1982). https://doi.org/10.1515/hfsg.1982.36.6.275

Laurichesse, S., Avérous, L.: Chemical modification of lignins: towards biobased polymers. Prog. Polym. Sci. **39**(7), 1266–1290 (2014)

Lee, S.H., Doherty, T.V., Linhardt, R.J., Dordick, J.S.: Ionic liquid-mediated selective extraction of lignin from wood leading to enhanced enzymatic cellulose hydrolysis. Biotechnol. Bioeng. **102**(5), 1368–1376 (2009)

Lee, W., Chang, K., Tseng, I.: Properties of phenol-formaldehyde resins prepared from phenol-liquefied lignin. J. Appl. Polym. Sci. **124**(6), 4782–4788 (2012)

Li, J., Wang, W., Zhang, S., Gao, Q., Zhang, W., Li, J.: Preparation and characterization of lignin demethylated at atmospheric pressure and its application in fast curing biobased phenolic resins. RSC Adv. **6**(71), 67435–67443 (2016)

Li, J., Zhang, J., Zhang, S., Gao, Q., Li, J., Zhang, W.: Alkali lignin depolymerization under eco-friendly and cost-effective NaOH/urea aqueous solution for fast curing bio-based phenolic resin. Ind. Crops Prod. **120**, 25–33 (2018)

Matuana, L.M., Riedl, B., Barry, A.O.: Caracterisation cinetique par analyse enthalpique differentielle des resines phenol-formaldehyde a base de lignosulfonates. Eur. Polym. J. **29**(4), 483–490 (1993)

McElroy, R.D., Lai, K.: Fractionation-purification, IR, 1H 13C NMR spectral and property studies of an industrial based sludge lignin. J. Wood Chem. Technol. **8**(3), 361–378 (1988)

Monteil-Rivera, F., Phuong, M., Ye, M., Halasz, A., Hawari, J.: Isolation and characterization of herbaceous lignins for applications in biomaterials. Ind. Crops Prod. **41**, 356–364 (2013)

Neiss, T.G., Vanderheiden, E.J.: Solution and solid-state NMR analysis of phenolic resin cure kinetics. Macromol. Symp. **86**(1), 117–129 (1994)

Pan, X., Kadla, J.F., Ehara, K., Gilkes, N., Saddler, J.N.: Organosolv ethanol lignin from hybrid poplar as a radical scavenger: relationship between lignin structure, extraction conditions, and antioxidant activity. J. Agric. Food Chem. **54**(16), 5806–5813 (2006)

Penkina, A., et al.: Solid-state properties of softwood lignin and cellulose isolated by a new acid precipitation method. Int. J. Biol. Macromol. **51**(5), 939–945 (2012)

Pilato, L.: Phenolic resins: a century of progress, vol. 11. Springer, Berlin (2010). https://doi.org/10.1007/978-3-642-04714-5

Poljansek, I., Krajnc, M.: Characterization of phenol-formaldehyde prepolymer resins by in line FT-IR spectroscopy. Acta Chim. Slov. **52**(3), 238 (2005)

Qin, Y., Meng, F., Xu, C., Hu, Z., Zhang, Y., Jia, Y., Yuan, X.: Preparation and performance of novel flavonoid phenols-based biomass-modified phenol formaldehyde resins. J. Inorg. Org. Polym. Mater. (2023). https://doi.org/10.1007/s10904-023-02619-7

Ragauskas, A.J., et al.: Lignin valorization: improving lignin processing in the biorefinery. Science **344**, 1246843 (2014). https://doi.org/10.1126/science.1246843

Re, R., Pellegrini, N., Proteggente, A., Pannala, A., Yang, M., Rice-Evans, C.: Antioxidant activity applying an improved ABTS radical cation decolorization assay. Free Radic. Biol. Med. **26**(9–10), 1231–1237 (1999)

Rego, R., Adriaensens, P.J., Carleer, R.A., Gelan, J.M.: Fully quantitative carbon-13 NMR characterization of resol phenol–formaldehyde prepolymer resins. Polymer (Guildf) **45**(1), 33–38 (2004)

Robert, D., Mollard, A., Barnoud, F.: 13C NMR qualitative and quantitative study of lignin structure synthesized in *Rosa glauca* calluses. Plant Physiol. Biochem. **27**, 297–304 (1989)

Rocca, D.M., Vanegas, J.P., Fournier, K., Becerra, M.C., Scaiano, J.C., Lanterna, A.E.: Biocompatibility and photo-induced antibacterial






Journal : Large 43538 | Article No : 388 | Pages : 17 | MS Code : 388 | Dispatch : 21-1-2025

activity of lignin-stabilized noble metal nanoparticles. RSC Adv. **8**(70), 40454–40463 (2018)
Saake, B., Lehnen, R.: Lignin. Ullmann's Encycl. Indus. Chem. (2007). https://doi.org/10.1002/14356007.a15_305.pub3
Sadeghifar, H., Wells, T., Le, R.K., Sadeghifar, F., Yuan, J.S., Jonas Ragauskas, A.: Fractionation of organosolv lignin using acetone: water and properties of the obtained fractions. ACS Sustain. Chem. Eng. **5**(1), 580–587 (2017). https://doi.org/10.1021/acssuschemeng.6b01955
Sarkar, S., Adhikari, B.: Lignin-modified phenolic resin: synthesis optimization, adhesive strength, and thermal stability. J. Adhes. Sci. Technol. **14**(9), 1179–1193 (2000)
Scholze, B., Hanser, C., Meier, D.: Characterization of the water-insoluble fraction from fast pyrolysis liquids (pyrolytic lignin): part II. GPC, carbonyl goups, and 13C-NMR. J. Anal. Appl. Pyrolysis **58**, 387–400 (2001)
Serrano, L., Egües, I., Alriols, M.G., Llano-Ponte, R., Labidi, J.: Miscanthus sinensis fractionation by different reagents. Chem. Eng. J. **156**(1), 49–55 (2010)
Sjöholm, R., Holmbom, B., Akerback, N.: Studies of the photodegradation of spruce lignin by NMR spectroscopy. J. Wood Chem. Technol. **12**(1), 35–52 (1992)
Tejado, A., Pena, C., Labidi, J., Echeverria, J.M., Mondragon, I.: Physico-chemical characterization of lignins from different sources for use in phenol–formaldehyde resin synthesis. Bioresour. Technol. **98**(8), 1655–1663 (2007)
Thring, R.W., Chornet, E., Overend, R.P.: Recovery of a solvolytic lignin: effects of spent liquor/acid volume ratio, acid concentration and temperature. Biomass **23**(4), 289–305 (1990)
Thring, R.W., Vanderlaan, M.N., Griffin, S.L.: Fractionation of Alcell lignin by sequential solvent extraction. J. Wood Chem. Technol. **16**(2), 139–154 (1996). https://doi.org/10.1080/02773819608545815
Tian, R., Liu, Q., Zhang, W., Zhang, Y.: Preparation of lignin-based hydrogel and its adsorption on Cu 2+ ions and Co 2+ ions in wastewaters. J. Inorg. Organomet. Polym. Mater. **28**, 2545–2553 (2018)
Toledano, A., Serrano, L., Garcia, A., Mondragon, I., Labidi, J.: Comparative study of lignin fractionation by ultrafiltration and selective precipitation. Chem. Eng. J. **157**(1), 93–99 (2010)
Tribot, A., et al.: Wood-lignin: supply, extraction processes and use as bio-based material. Eur. Polym. J. **112**, 228–240 (2019). https://doi.org/10.1016/J.EURPOLYMJ.2019.01.007
Trosa, A., Pizzi, A.: A no-aldehyde emission hardener for tannin-based wood adhesives for exterior panels. Holz Als Roh-und Werkst. **59**(4), 266–271 (2001)
Van Dong, P., Ha, C.H., Binh, L.T., Kasbohm, J.: Chemical synthesis and antibacterial activity of novel-shaped silver nanoparticles. Int. Nano Lett. **2**, 1–9 (2012)
Vanholme, R., Demedts, B., Morreel, K., Ralph, J., Boerjan, W.: Lignin biosynthesis and structure. Plant Physiol. **153**(3), 895–905 (2010). https://doi.org/10.1104/pp.110.155119
Vattem, D.A., Lin, Y.-T., Labbe, R.G., Shetty, K.: Phenolic antioxidant mobilization in cranberry pomace by solid-state bioprocessing using food grade fungus *Lentinus edodes* and effect on antimicrobial activity against select food borne pathogens. Innov. Food Sci. Emerg. Technol. **5**(1), 81–91 (2004)
Vlietinck, A.J., Vanden Berghe, D.A.: Can ethnopharmacology contribute to the development of antiviral drugs. J. Ethnopharmacol. **32**(1–3), 141–153 (1991)
Watkins, D., Nuruddin, M., Hosur, M., Tcherbi-Narteh, A., Jeelani, S.: Extraction and characterization of lignin from different biomass resources. J. Mater. Res. Technol. **4**(1), 26–32 (2015)
Werstler, D.D.: Quantitative 13C nmr characterization of aqueous formaldehyde resins: 1. Phenol-formaldehyde resins. Polymer (Guildf) **27**(5), 750–756 (1986)
Yang, H., Yan, R., Chen, H., Lee, D.H., Zheng, C.: Characteristics of hemicellulose, cellulose and lignin pyrolysis. Fuel **86**(12–13), 1781–1788 (2007)
Yang, S., Zhang, Y., Yuan, T., Sun, R.: Lignin–phenol–formaldehyde resin adhesives prepared with biorefinery technical lignins. J. Appl. Polym. Sci. (2015). https://doi.org/10.1002/app.42493
Yi, Z., Zhang, J., Zhang, S., Gao, Q., Li, J., Zhang, W.: Synthesis and mechanism of metal-mediated polymerization of phenolic resins. Polymers (Basel) **8**(5), 159 (2016)
Zakzeski, J., Bruijnincx, P.C.A., Jongerius, A.L., Weckhuysen, B.M.: The catalytic valorization of lignin for the production of renewable chemicals. Chem. Rev. **110**(6), 3552–3599 (2010)
Zhang, W., Ma, Y., Wang, C., Li, S., Zhang, M., Chu, F.: Preparation and properties of lignin–phenol–formaldehyde resins based on different biorefinery residues of agricultural biomass. Ind. Crops Prod. **43**, 326–333 (2013)
Zhao, L., Ouyang, X., Ma, G., Qian, Y., Qiu, X., Ruan, T.: Improving antioxidant activity of lignin by hydrogenolysis. Ind. Crops Prod. **125**, 228–235 (2018)

| | |
|---|---|
| Journal: | **43538** |
| Article: | **388** |

# Author Query Form

**Please ensure you fill out your response to the queries raised below and return this form along with your corrections**

Dear Author

During the process of typesetting your article, the following queries have arisen. Please check your typeset proof carefully against the queries listed below and mark the necessary changes either directly on the proof/online grid or in the 'Author's response' area provided below

| Query | Details Required | Author's Response |
|---|---|---|
| AQ1 | Table 1 was mentioned twice, so we have renumbered the second occurrence as Table 3. Kindly check and confirm. | |
| AQ2 | Please check and confirm the inserted citation of Fig. 12 and Tables 2 to 4 are correct. If not, please suggest an alternative citation. Please note that figures and tables should be cited in sequential order in the text. | |
| AQ3 | References (He and Yan 2005, Kuroe et al. 2013, Yang et al. 2015) are given in list but not cited in text. Please cite in text or delete from list. | |
| AQ4 | Inclusion of a data availability statement is preferred for this journal. If applicable, please provide one. | |
| AQ5 | As per journal instructions Competing Interests is required for this article, kindly check and confirm. | |